BULLETIN OF THE EARTHQUAKE
RESEARCH INSTITUTE
Vol. 57 (1982), pp. 627-652

29. *Accuracy of the Initial Phase and the Phase Velocity of Surface Waves with Special Reference to the Single-Station Method.*

By Mitsuru YOSHIDA,

Earthquake Research Institute.

(Received October 29, 1982)

Abstract

Initial phase of surface waves, which depends on such earthquake source parameters as depth, source-type and -orientation, source time function and medium property near the source, is investigated specially with respect to accuracy. The effects of small errors in the solution of the earthquake mechanism and uncertainties of the local underground structure near the source region on the initial phase of surface waves are quantitatively examined on the basis of the dislocation theory. By assuming the errors of source parameters and by using different medium models, the errors of the initial phase and surface wave velocity are evaluated. Against an error of $\pm 5^\circ$ in the dip and slip angles of the fault plane at the source, the space phase error in the initial phase is negligible in most parts of the azimuth except the minimum amplitude direction. Against an error of the source time function, the phase error of 0.1 radian or so may be caused at the period 40 sec and it decreases as the period increases. If we assume an earthquake with the magnitude 6 to be a point source, a phase error of maximum 0.4 radian in the initial phase due to the finite fault length will be produced at the azimuth just opposite to the rupture direction. It can be said that the space phase error due to uncertainties of the medium property near the source is negligible as far as we use a reasonable model representing the source region. Among the three phase factors of the initial phase, the error of the rupture propagation phase is largest, and the initial phase error decreases as the period increases. The total error of the initial phase seems not to exceed 0.6 radian at the period 40 sec and 0.3 radian at 100 sec, when an earthquake with the magnitude 6 or less is used and the station is carefully chosen in order to select the azimuth of the stable portion of the initial phase, by taking the amplitude radiation pattern of surface waves at the source into consideration. For an error in the initial phase of 0.6 radian at the periods 40 and 100

sec, for the path length of about 9000 km, the phase velocity error of Rayleigh waves is estimated to be 0.007 km/sec (0.17%) and 0.018 km/sec (0.44%) respectively.

1. Introduction

The single-station method, which determines the phase velocity of surface waves for the great circle path between the epicenter and the station, was proposed by BRUNE, NAFE and OLIVER (1960), and this method was applied to the phase velocity determination in the Pacific (KUO, BRUNE and MAJOR, 1962) for the period range from 20 to 140 sec. In those works, the method of stationary phase was applied to the single-station method, and phase velocities were determined by assuming the initial phase to be independent of period and by chosing the initial phase so that the phase velocity curve agrees in the long period range with the phase velocity curve of the mantle wave. However, it was also reported that the surface waves have a frequency-dependent initial phase which is a function of the focal mechanism and the structures of the earth (SATÔ, 1960; KNOPOFF and SCHWAB, 1968).

Due to the establishment of the earthquake dislocation theory (*e. g.*, MARUYAMA, 1963) and the excitation theory of surface waves (*e. g.*, SAITO, 1967; HARKRIDER, 1970), the space phase is now determined reasonably. Making use of synthetic seismograms, the azimuthal variation of the space phase has been investigated by ODAKA and USAMI (1970). The study on phase velocity dispersion of surface waves in the Pacific, which was done earlier by KUO, BRUNE and MAJOR (1962), is carried on by means of the refined single-station method. The phase velocity data obtained by KAUSEL, LEEDS and KNOPOFF (1974), LEEDS (1975), and FORSYTH (1975a, b) were used for the study of the structure under the Pacific (LEEDS, KNOPOFF and KAUSEL, 1974; SCHLUE and KNOPOFF, 1976, 1977).

Although the accuracy of the single-station method has been studied by YOSHIDA (1977), the examination is rather qualitative, and the discussions including the phase velocity are desirable so that the single-station method might be exployed effectively in the future. If we can understand the error range of the initial phase caused by several factors, the phase velocity of surface waves would be greatly utilized for the study of the structures of the earth.

2. Characteristics of the initial phase of surface waves

The initial phase of surface waves consists of three factors (BEN-

MENAHEM and TOKSÖZ, 1963); 1) the space phase depending on the force system exerted at the source, 2) the rupture propagation phase arising from the assumption that the rupture is propagated horizontally over a finite length with a certain velocity, and 3) the time phase which comes from the source time history. These factors can be calculated if the earthquake source mechanism and the underground structure near the source are given. The first two factors depend on both of the wave period and the medium property near the source. On the other hand the last factor does not directly depend on the medium, though it is pointed out that the source time function is strongly affected by the physical condition of the medium where the initial stress is exerted (YAMASHITA, 1978) or the dynamic frictional conditon at the fault surface (OHNAKA, 1973).

In YOSHIDA (1977) the phase velocity of Love waves across the Pacific was determined by using the Shikotan earthquake of 1968 which occurred off the northeast coast of Hokkaido. The space and rupture propagation phases were calculated by using an oceanic model, and the initial phase of Love waves which varies with the period was shown. However, a rigorous check was not carried out to see whether the medium model used was appropriate or not for the calculation of the initial phase.

The space phase is determined by using the surface wave radial factors of the displacement- and the stress-components at the layer where the seismic source is located, and the behavior of the factors in the earth depends on the physical properties of the crustal or mantle materials. In the propagation phase Love or Rayleigh wave velocities near the source are directly related to the phase characteristic. In YOSHIDA (1977), for the calculation of the space and rupture propagation phases, the radial factors of the displacementand stress-components presented by HARKRIDER (1970) using Thomson-Haskell method for the Anderson-Toksöz' oceanic model were used.

In order to understand the characteristics of the space and rupture propagation phases which are a function of the medium, a couple of oceanic upper mantle models were examined, in which the phases were calculated through the formula (SAITO, 1967) of the surface wave excitation.

3. Earthquake data used for determining Rayleigh wave phase velocity

To examine the accuracy of the initial phase of surface waves, previously detemined initial phase of Love wave and newly calculated one

of Rayleigh wave were considered, both Love and Rayleigh waves being excited by the Shikotan earthquake. The source parameters of this earthquake reported by SHIMAZAKI (1975) were adopted for the calculation of the individual phase factor, as was done in the previous work.

The hypocenter elements of the earthquake reported by USGS and ISC are listed in Table 1 together with the station locations belonging to the World Wide Standard Seismograph Network (WWSSN). A wave train of Rayleigh waves was recorded on the WWSSN long-period seismograph at the station RAR (Rarotonga, Cook Island) in a satisfactory form (Fig.

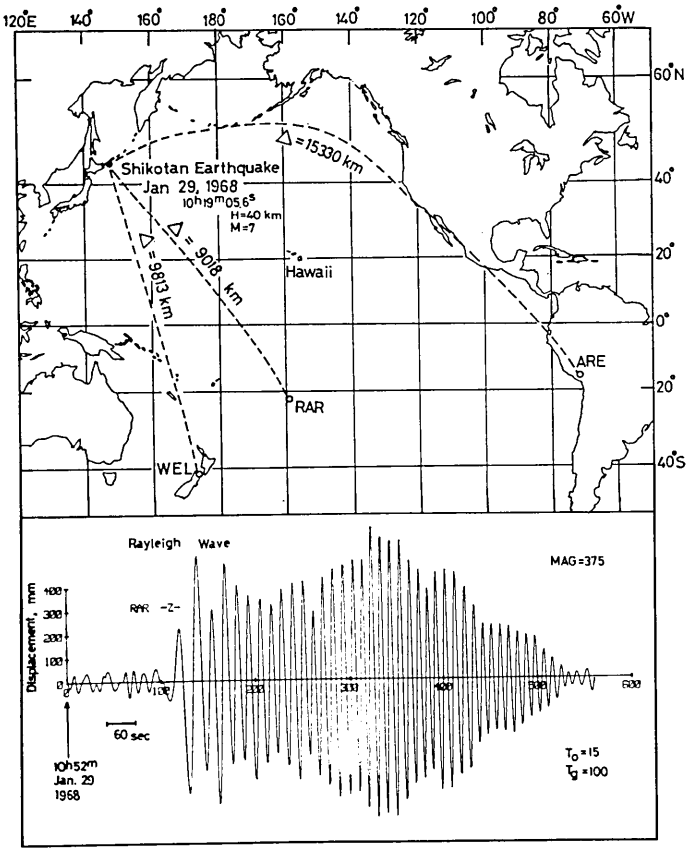

Fig. 1. Top: Map of the locations of the epicenter of the Shikotan earthquake of 1968 and the stations. Bottom: The original wave form of Rayleigh waves of the vertical component observed at the station RAR, as recorded on the WWSSN seismograph (The free periods of the pendulum and galvanometer are 15 and 100 sec respectively). The unit 100 in the ordinate corresponds to 1 cm of the displacement on seismograms. Numerals under the abscissa are the sequential data numbers sampled at an interval 1.92 sec.

Table 1. Hypocentral elements of the Shikotan earthquake of 1968 reported by USGS and ISC, and the location of the three stations.

Shikotan Earthquake

	Date	Origin Time	Latitude	Longitude	Depth	Magnitude
USGS	Jan 29, 1968	$10^h19^m05.6^s$	43.6°N	146.7°E	40 km	7
ISC	Jan 26, 1968	$10^h19^m02.9^s$	43.52°N	146.72°E	20 km	6.3

Station

Code	Region	Latitude	Longitude
RAR	Rarotonga, Cook Island	21.217°S	159.773°W
ARE	Arequipa, Peru	16.462°S	71.491°W
WEL	Wellington, New Zealand	41.287°S	174.767°E

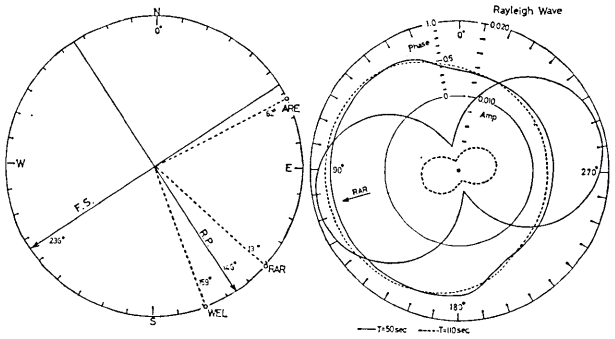

Fig. 2. Right: Amplitude radiation pattern and space phase of Rayleigh waves at the period of 50 and 110 sec. The direction towards RAR is indicated by an arrow. Left: Geometry of the direction of the fault strike (F.S.) and the rupture propagation (R.P.), and of the station locations. Numerals in the circle indicate the azimuthal angles measured from the north.

1). The magnification of the seismograph at RAR was 375, rather low, and it was appropriate for the present analysis. The station RAR was just located in the direction of the rupture propagation of the Shikotan earthquake (Fig. 2).

4. Method for calculating the space phase of Rayleigh and Love waves

The space phase depending on the force system was calculated as follows. At the source we assume that the double couple of body forces is exerted and the time dependence is forming of an impulse. According to SAITO (1967), the vertical component of the displacement of Rayleigh

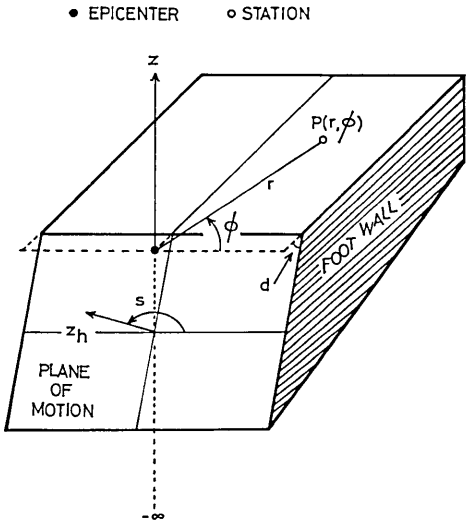

Fig. 3. Fault plane geometry and coordinate system.

wave at $P(r, \phi)$ in the cylindrical coordinate system (r, ϕ, z) is written as follows: (r is the epicentral distance; ϕ is the station azimuth measured counterclockwise from the strike of the fault plane; z axis points upwards, see Fig. 3)

$$u^R(r, \phi) = \frac{1}{2}\int_0^\infty \frac{y_1(0)}{4\pi c U I_1{}^R} \cdot \chi_h{}^R(\phi, z_h, k) \cdot \sqrt{\frac{2}{\pi k r}} \cdot e^{i(pt - kr + (3/4)\pi)} dp\,, \qquad (1)$$

where

$$\begin{aligned}\chi_h{}^R(\phi, z_h, k) = k y_1(z_h)\Big(&-\frac{3\lambda+2\mu}{\lambda+2\mu}\cdot\frac{1}{2}\cdot\sin s \sin 2d\Big)\\ &+\frac{1}{2}\sin 2d \sin s \cos 2\phi - \sin d \cos s \sin 2\phi\\ &-\frac{y_2(z_h)}{\lambda+2\mu}\sin s \sin 2d\\ &-\frac{y_4(z_h)}{\mu} i(\cos d \cos\phi + \sin s \cos 2d \sin\phi)\,.\end{aligned} \qquad (2)$$

The notations s and d are the slip and dip angles of the fault plane, and c and U are the phase and group velocities respectively at the augular frequency $p(=ck)$. The source is located at the layer z_h, and λ and μ are the Lame's constants at z_h.

$I_1{}^R$ in equation (1) is defined as

$$I_1{}^R = \int_{-\infty}^0 \rho(z)[y_1{}^2(z) + y_3{}^2(z)]dz\,, \qquad (3)$$

where ρ is the density. $y_1(z), y_2(z), y_3(z)$ and $y_4(z)$ are the normal mode solutions satisfying the equations

$$\begin{aligned}
\frac{dy_1}{dz} &= \frac{1}{\lambda+2\mu} y_2 + \frac{k\lambda}{\lambda+2\mu} y_3 , \\
\frac{dy_2}{dz} &= -k^2c^2\rho y_1 + k y_4 , \\
\frac{dy_3}{dz} &= -k y_1 + \frac{1}{\mu} y_4 , \\
\frac{dy_4}{dz} &= -\frac{k\lambda}{\lambda+2\mu} y_2 - \frac{k^2c^2\rho + [4k^2\mu(\lambda+2\mu)]}{\lambda+2\mu} y_3 ,
\end{aligned} \tag{4}$$

and the boundary conditions

$$\begin{aligned}
&y_2(0)=y_4(0)=0 , \\
&y_1(-\infty)=y_2(-\infty)=y_3(-\infty)=y_4(-\infty)=0 .
\end{aligned} \tag{5}$$

From the expressions (1) and (2) the space phase of Rayleigh wave can be written as

$$\phi_h{}^R(p)=\arg \chi_h{}^R(\phi, z_h, k)+\frac{3}{4}\pi . \tag{6}$$

Similarly, the displacement due to Love wave can be written as

$$u^L(r, \phi)=\frac{1}{2}\int_0^\infty \frac{y_1(0)}{2cUI_1{}^L}\cdot\sqrt{\frac{2}{\pi kr}}\cdot\frac{1}{2\pi}\cdot\chi_h{}^L(\phi, z_h, k)\cdot e^{i(pt-kr-(3/4)\pi)}dp , \tag{7}$$

where

$$\begin{aligned}
\chi_h{}^L(\phi, z_h, k)=\frac{p}{c}y_1(z_h)[&\sin d\cos s\cos 2\phi+\frac{1}{2}\sin 2d\sin s\sin 2\phi \\
&+i\frac{y_2(z_h)}{\mu}[\sin s\cos 2d\cos\phi-\cos d\cos s\sin\phi] .
\end{aligned} \tag{8}$$

$I_1{}^L$ in equation (7) is defined by

$$I_1{}^L=\int_{-\infty}^0 \rho(z)y_1{}^2(z)dz . \tag{9}$$

$y_1(z)$ and $y_2(z)$ in equations (7), (8) and (9) are the normal mode solutions satisfying the following differential equantions

$$\begin{aligned}
\frac{dy_1}{dz} &= \frac{1}{\mu} y_2 , \\
\frac{dy_2}{dz} &= k^2(\mu-c^2\rho)y_1 ,
\end{aligned} \tag{10}$$

and the boundary conditions

$$y_2(0)=0\,,$$
$$y_1(-\infty)=y_2(-\infty)=0\,. \tag{11}$$

Consequently from (7) and (8) the spase phase of Love wave can be written as

$$\phi_h{}^L(p)=\arg \chi_h{}^L(\phi, z_h, k)-\frac{3}{4}\pi\,. \tag{12}$$

The normal mode solutions of Rayleigh or Love waves are determined by solving the differential equations (3) and (4) or (10) and (11) by means of numerical integrations.

The space phase of Love wave expressed in the equation (12) has the same form as the one written in YOSHIDA (1977). Hereafter the formulas (6) and (12) are employed for the calculation of the space phase of Rayleigh and Love waves.

4.1. Effect of the underground structure upon the space phase

For Rayleigh waves the space phase was calculated for the four upper mantle models 1) PC-MAX corresponding to the region of the ocean-floor age of 150 m. y. or more, 2) PC-MIN corresponding to the region of 0 m. y., 3) 8099-80 corresponding to the region of 90-150 m. y., 4) OC corresponding to an average oceanic region which is compared with an average continental region. PC-MAX, PC-MIN and 8099-80 were constructed from Rayleigh wave dispersion data in the Pacific (the first two are introduced by YOSHIDA (1978); the third by YOSHII (1975). OC was constructed by Anderson and Toksöz (see in detail HARKRIDER, 1970) and used by YOSHIDA (1977) for the calculation of the initial phase of Love waves. For Love waves the space phase was calculated for three models 1) PC-MAX, 2) PC-MIN and 3) OC.

The space phases of Rayleigh and Love waves calculated for the direction of ARE, RAR and WEL (see Table 1) are shown in Fig. 4. This figure shows that the characteristics of the space phase of Rayleigh waves for PC-MAX and 8099-80 are very close for the directions 174° (ARE), 105°(RAR) and 77°(WEL), and the phase difference between PC-MAX and 8099-80 is less than 0.03 radian in the period range from 40 to 150 sec. However the phase characteristics for OC and PC-MIN are somewhat different from those for PC-MAX and 8099-80, the maximum difference amounting to 0.1 radian. These phase characteristics suggest that the oceanic models for the west Pacific may give the proper space phase of Rayleigh waves when they are excited by earthquakes occurring around the west Pacific.

We also see from Fig. 4 that the space phase of Love waves for OC

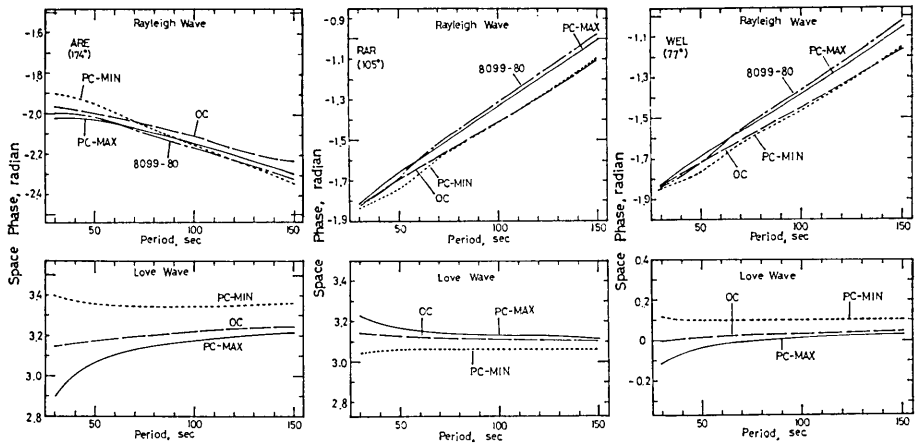

Fig. 4. Space phase of Rayleigh and Love waves at the stations ARE, RAR and WEL, calculated for the upper mantle models PC-MIN, OC, 8099-80 and PC-MAX. Numerals in the parentheses under the station code show the azimuthal angles measured counterclockwise from the fault strike.

lies between those for PC-MAX and PC-MIN, and it is rather close to the former than to the latter. The difference of the space phase between OC and PC-MIN approaches 0.2 radian at the period 40 sec for ARE and it is about 0.1 radian at 150 sec, twice those between PC-MAX and OC at the two periods respectively.

The model PC-MIN corresponds rather to the region near the East Padific Rise and, in the case of the Shikotan earthquake, seems to cause a larger error for the space phase calculation of Love waves, as was so for Rayleigh waves. For earthquakes near the west Pacific PC-MAX and OC may be safely applied to the determination of the Love wave space phase. A large space phase difference between PC-MIN and PC-MAX for ARE, approximately twice of those for RAR and WEL, indicates that the space phase greatly depends on the azimuth of the station measured from the strike of the fault.

4.2. Effect of the source parameters upon the space phase

The focal mechanism of an earthquake is generally solved by the polarity of up or down of the first motion of P wave, the polarization angle of S wave, the radiation pattern of surface wave, however the fault plane cannot be determined uniquely without other seismological data, such as the distribution of aftershocks. It can be said that the accuracy in the focal mechanism solution increases if the solution is determined by using various kinds of seismological data. However, we are sometimes

compelled to use the data involving a little noise, causing severe errors. Errors are also produced in the data handling. Those errors directly influence the accuracy of the source informations such as the fault-type, -orientation, -length, and the source time function.

The solution of the slip motion of the Shikotan earthquake is that the slip angle is 107°(=s), with the fault plane dipping downwards in the low angle of 23°(=d). Shallow earthquakes having such a fault type often occur near the subduction zone of the Pacific plate and they are used as the data source of the velocity determination of surface waves propagating in the Pacific.

The space error due to source parameter errors of the slip and dip angles were estimated by changing the individual angle to a small extent, and the variation of the space phase error is shown in Fig. 5. The small

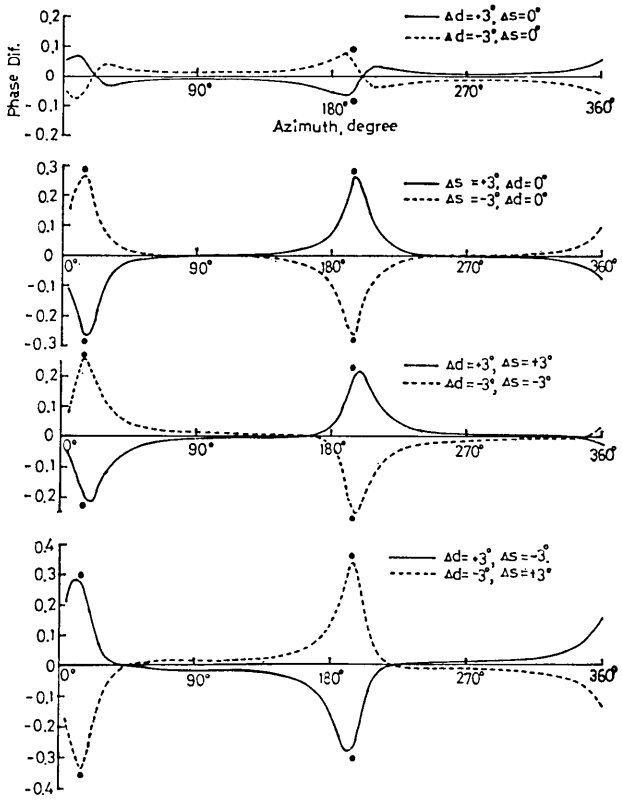

Fig. 5. Space phase difference due to the small error of the dip angle d and the slip angle s for the focal mechanism solution of d=23° and s=107°. The azimuth measured counterclockwise from the fault strike ranges from 0° to 360°. Solid circles show the minimum amplitude azimuth.

error within $\pm 3°$ will be mostly involved in the source orientation solution though the error of $\pm 5°$ seems to give an upper limit.

We notice from Fig. 5 that the effect due to the errors of the dip and slip angles is quite negligible in a large part of the azimuth. According to Fig. 2 the minimum amplitude azimuth is located at 15° and 195°, and the phase characteristics vary rapidly at those azimuths. This phase variation near the minimum amplitude azimuth is larger at the short period than at the long period (See Fig. 4). Comparing the effect due to the errors of the dip (Δd) and slip (Δs) angles, the former is about one fourth less space phase error than the latter, (upper two in Fig. 5). It can be also understood that, for earthquakes of a low-angle thrust fault type such as the Shikotan earthquake, the space phase error due to the error of $\pm 3°$ of the combination of the dip and slip angles is at most 0.03 radian except near the minimum amplitude azimuth. (lower two in Fig. 5).

5. Accuracy of the rupture propagation phase

The propagation phase, which arises from the assumption that the rupture is moving horizontally along the fault is determined through the expression (BEN-MENAHEM, 1961)

$$\phi_p{}^{R,L}(p)=-\frac{bp}{2c^{R,L}(p)}\left(\frac{c^{R,L}(p)}{v}-\cos\theta\right) \tag{13}$$

where the superscripts R and L correspond to Rayleigh and Love waves respectively, and

$c^{R,L}(p)$: phase velocity of Rayleigh and Love waves near the source
b : fault length
v : rupture velocity
p : angular frequency
θ : angle between the direction of rupture propagation and the station, measured counterclockwise.

5.1. Effect of the underground structure upon the propagation phase

As was examined in the space phase, the propagation phase was calculated, in the order of decreasing ocean-floor age, for PC-MAX, 8099-80, OC and PC-MIN for Rayleigh waves, and for Love waves, PC-MAX, OC and PC-MIN were considered (Fig. 6). For the Shikotan earthquake, the rupture direction is N146°S (Fig. 2) and the fault parameters, length 80 km and rupture velocity 3 km/sec, are used for the calculation. The ex-

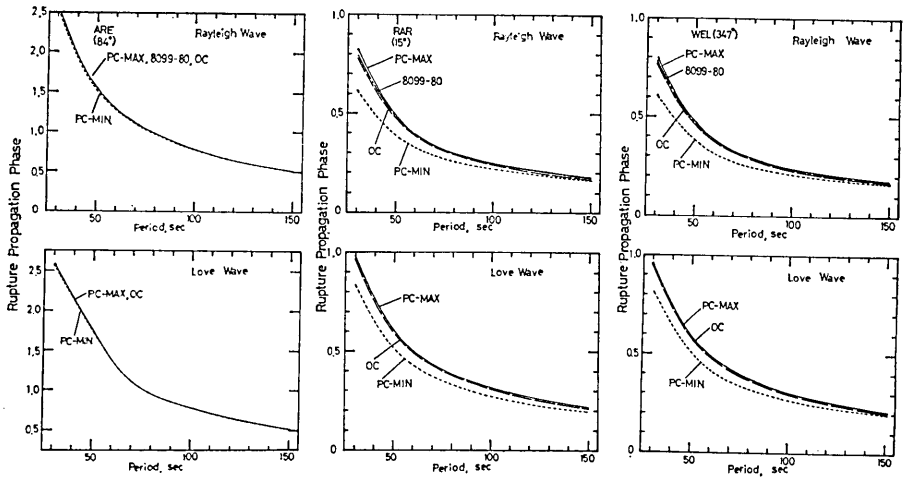

Fig. 6. Rupture propagation phase of Rayleigh and Love waves for the fault length 80 km and the rupture velocity 3 km/sec for the period ranging from 30 to 150 sec, calculated for the upper mantle models PC-MAX, 8099-80, OC and PC-MIN. Numerals in the parentheses under the station code show the azimuthal angle measured counterclockwise from the direction of the rupture propagation.

pression (13) shows that the coefficient depending on the medium is only the phase velocity of Rayleigh and Love waves near the source, which can be calculated if the medium model near the source is given.

According to Fig. 6, the propagation phase of both Rayleigh and Love waves calculated for PC-MAX, 8099-80 and OC are very close for three stations, ARE, RAR and WEL. The difference between them is less than 0.02 radian. It is expected that the propagation phases for RAR and WEL have similar characteristcs since two stations are located nearly in the same direction (See Fig. 2). Fig. 6 also shows that the propagation phase for PC-MIN except for ARE differs from those for other models, by about 0.1 radian at the period 50 sec and by about 0.01 or 0.02 radian at 150 sec, while for ARE the propagation phase is extremely close to those for all the models. This phenomenon can be interpreted as that the azimuthal term of ARE in (13) is very small, and the expression is nearly equal to $bp/(2v)$, which is only a function of the wave period.

5.2. Effect of the fault length upon the propagation phase

According to the expression (13), if the fault length is small the rupture propagation phase becomes small. In this section the relationship between the earthquake megnitude and the propagation phase is examined in detail. For this purpose we must know the relation between the

magnitude of the earthquake and the fault length. It is evident that generally the larger the magnitude of earthquake is, the longer the fault becomes (*e. g.*, TOCHER, 1958; IIDA, 1959, 1965; PRESS, 1967; WYSS and BRUNE, 1968). However the relation between them is not so strict but has large scattering.

The difficulty may arise from the situation that earthquakes do not necessarily on the ground surface, but there are hidden parts under the crust. The aftershock area often gives data for inferring the fault length, though an overestimation is likely to occur (AKI, 1968). For the estimation of the fault length, we can apply the "ω-square model" (AKI, 1967, 1972) indicating that the source spectrum is proportional to ω^{-2} beyond the corner frequency, the spectral intensity being proportional to the seismic moment and being flat below the frequency, where ω is an angular frequency (AKI, 1966).

According to the above model, the fault length b should be proportional to the corner period T,

$$b=cT\,, \tag{14}$$

where a value of 0.65 km/sec for the constant c gives the best fit to the observation. Based on this relation AKI (1967) showed the relation between the magnitude and the fault length, the fault length of 80, 30, 10, 6.4 and 3 km corresponding to the magnitude of approximately 7.6, 7.2, 6.3, 6.0 and 4.9 respectively. The rupture propagation phase as a function of the fault length was calculated through the expression (13) using the phase velocity $c^{R,L}(p)$ (Fig. 7) for the model 8099-80 corresponding to the region of the west Pacific and is shown in Fig. 8.

From Fig. 8 we see that the propagation phase between Rayleigh and Love waves are very similar. The phase delay for the period of 40 sec is maximum just at the opposite direction of the rupture propagation (0.14, 0.27 and 0.45 radian for the fault length of 3, 6, and 10 km respectively at the azimuth of 180°), and is minimum at the rupture direction. The longer the period is the smaller the phase delay due to the rupture propagation becomes.

We notice that if the single-station method is employed for the earthquake of magnitude from 5 to 6, the phase error due to the disregard of the propagation term is at most 0.3 radian for both Rayeligh and Love waves. This phase delay of 0.3 radian corresponds to the time delay of 1.5 and 5 sec for the period 30 and 100 sec respectively. In the azimuthal range within $\pm 90°$ measured from the rupture direction the phase delay is less than 0.2 radian even if the fault length reaches 10 km, for the

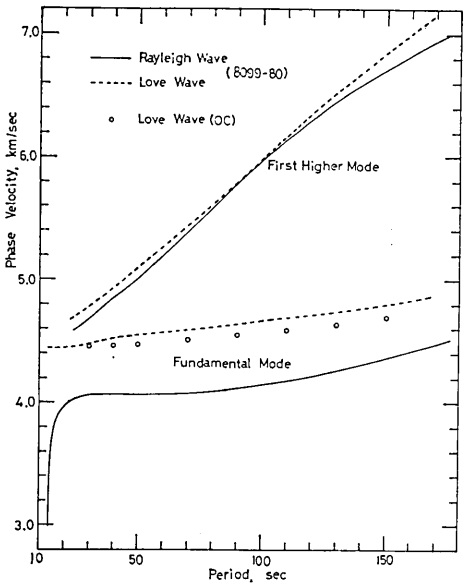

Fig. 7. Phase velocities of Rayleigh and Love waves of the fundamental and first higher modes calculated for the model 8099-80, with the velocities corrected for the effect of the sphericity of the earth's layering. Open circles mean the phase velocity for the model OC. Velocities of the first higher mode are shown merely for reference.

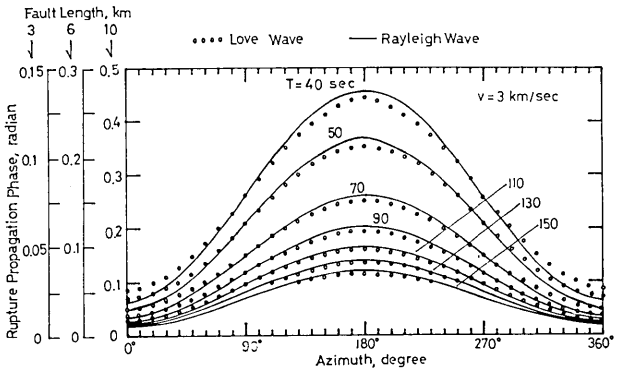

Fig. 8. Rupture propation phase of Rayleigh (solid lines) and Love (open circles) waves for the fault length of 3, 6 and 10 km, and the rupture velocity of 3 km/sec. The azimuthal angle is measured counterclockwise from the direction of the rupture propagation. Parameter is the wave period (T).

period longer than 40 sec (Fig. 8).

In order to understand the effect of the longer fault length, the propagation phase of the Shikotan earthquake was calculated at the directions 15° (RAR), 84° (ARE) and 347° (WEL) and is shown in Fig. 9 for various values of b. The fault length of this earthquake is reported to be 80 km (SHIMAZAKI, 1975), and at the station ARE located nearly perpendicular to the rupture direction the phase value exceeds 1 radian for the periods shorter than 80 sec for both Rayleigh and Love waves. However, the rupture propagation phase becomes small rapidly with decreasing fault length. If it is about 6 km, the propagation phase of Rayleigh and Love waves hardly exceeds 0.15 radian for the period longer than 40 sec. It can be said that for larger earthquakes the propagation phase greatly contributes to the initial phase of surface waves.

As to the rupture propagation phases for Rayleigh and Love waves, at the stations RAR and WEL which are closely located to the rupture direction 0°, the former is 0.1 radian less than the latter for the fault length 80 km in the period range from 40 to 100 sec (Fig. 9), corresponding to phase velocity of 0.4 km/sec lower for Rayleigh waves than for Love waves (Fig. 7).

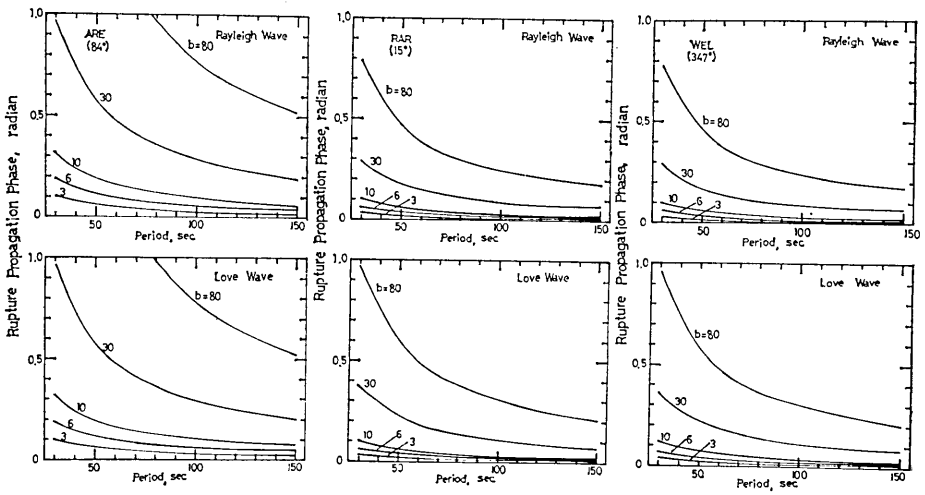

Fig. 9. Rupture propagation phase of Rayleigh and Love waves for the rupture velocity 3 km/sec and the fault length (b) of 80, 30, 10, 6 and 3 km for the period range from 30 to 150 sec. For numerals in the parentheses see the caption in Fig. 6.

6. Accuracy of the time phase

As a form of the force exerted at a seismic source, an impulsive force or a force varying as a step-function in time are often assumed. The phase characteristic of those source functions were examined by AKI (1962) with special reference to the earthquake mechanism. It was considered by MARUYAMA (1963) that, even for a moving dislocation source, the double couple systems distributed on the fault surface varies its strength with time in the form of an approximate step function, their outset shifting in accordance with the velocity and the direction of the dislocation propagation. It is also reported that the assumption of a step function is reasonable for large earthquakes such as the Kurile Island earthquake of 1963 or the Alasker earthquake of 1964 (KANAMORI, 1970a, b) by comparing synthetic surface waves with the observed ones at the long period range.

The ramp function, which is written as

$$m(t)=\begin{cases} 0 & t<0 \\ \dfrac{t}{T_0} & 0\leqq t\leqq T_0 \\ 1 & t>T_0 \end{cases} \tag{15}$$

or the function varying as

$$m(t)=1-\exp(-t/\tau) \qquad t\geqq 0 \tag{16}$$

are similar to the step-function and they are often used as the source time function. The phase characteristics of those functions are examined in YOSHIDA (1977). The time constants T_0 or τ in the expressions (15) and (16) usually depend on the magnitude of the earthquake and increase with increasing magnitude. The rise time T_0 of the Parkfield earthquake of June 28, 1966, which has a surface wave magnitude of 6.4 (WU, 1968) and a fault length of about 30-40 km (BROWN and VEDDER, 1967) and of 30 km (FILSON and MCEVILLY, 1967) was determined as 0.4-0.9 sec (AKI, 1968, 1972) or 0.5-0.7 (KAWASAKI, 1975). For smaller earthquakes with smaller earthquakes with magnitude 6 or less and with a fault length less than about 10 km it seems that the rise time does not exceed 1 sec (TSAI and AKI, 1970).

Usually in the single-station method the step-function is assumed at the source and the time phase of $-\pi/2$ radian is taken into the initial phase. Small difference of the time phase between the ramp function and the step function is caused (Fig. 10). The difference for the rise time of

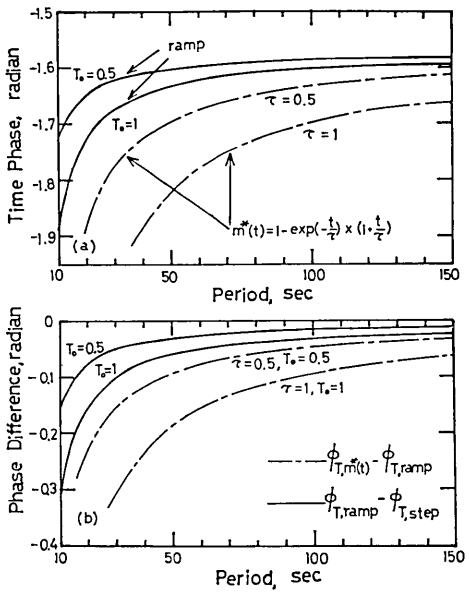

Fig. 10. Top: Time phase for the ramp function in (15) and the time function of the expression (17) in the text. Bottom: Time phase difference between the two time functions.

1 sec is about 0.07 radian at the period 40 sec and it decreases to 0.03 radian at 100 sec. Since these values are small they can be disregarded for the phase velocity determination for the period longer than 40 sec.

Up to now several theoretical investigations with regard to the source function have been carried out (*e. g.*, ARCHAMBEAU, 1968; BURRIDGE, 1969; HANSON *et al.*, 1971; and IDA and AKI, 1972). However in these studies it is somewhat difficult to infer directly the phase characteristics of the function since the form of the function is too complicated. A source time function which is somewhat different from the expresssions of (15) and (16) was proposed by OHNAKA (1973) from a view point of the dynamic characteristics of friction in the dislocation motion.

The form of the function is

$$m^*(t)=1-(1+t/\tau)\cdot\exp(-t/\tau) \qquad t\geqq 0 \tag{17}$$

where the time constant τ depends upon the propagating velocity of dislocation, the shear wave velocity and the width of the fault, and it was found that the estimated values for several earthquakes coincided well with the direct evaluation on the basis of the seismic wave data. YAMASHITA (1977) considered the earthquake rupture as the relaxation of a

nonuniformly accumulated initial stress or strain field and proposed a time function in a form similar to (17).

The phase component of the function expressed by (17) is written as

$$\phi_T(p)=-\pi+\tan^{-1}\left(\frac{1-p^2\tau^2}{2p\tau}\right), \tag{18}$$

which is calculated and is shown in Fig. 10, together with the phase angle of the ramp function. This figure indicates that the phase difference between the two time functions calculated for $\tau=1$ and $T_0=1$ sec is about 0.2, 0.1, and 0.06 radian at the period 50, 100, and 150 sec respectively. For $\tau=0.5$ and $T_0=0.5$ sec the difference becomes half. Here it should be noted that the rise time T_0 and the time constant τ are not equivalent.

At the present time it is hard to conclude which type of function is the best for representing the behaviour of the time dependence of the displacement at the seismic source. However, from Fig. 10 we can understand the if the source is the ramp function, the time phase error arising from the assumption of the phase angle of $-\pi/2$ is less than 0.1 radian, while if the source is represented by the expression (17) the time phase error is within about 0.2 radian, for the period longer than 40 sec, showing a slight increase.

7. Determination of phase velocity of Rayleigh waves by the single-station method

For eliminating the noise a wave train of Rayleigh waves observed at RAR (Fig. 1) was band-pass filtered by the use of the best filtering parameters (YOSHIDA, 1982), operated in terms of the Gaussian function in the frequency domain (DZIEWONSKI, BLOCH and LANDISMAN, 1969), and is shown in Fig. 11. The upper most seismogram is the original and the other shows the waves filtered every ten seconds from 10 to 100 sec, indicating the value of the maximum half amplitude for each wave train. We see from Fig. 11 that the seismic wave energy is prevailing in the short period around 20 sec and the energy seems to decrease with increasing period. We notice that the wave components appearing at the outset of the original wave train are those of the period near 40-50 sec. The ratio of the amplitude at 40 and 100 sec is about 12 (71.2/6.1), which will be corrected to 3(11.7/4) since the ratio of the amplitude response of the WWSSN long-period seismograph is about 4 for the same couple of periods. Hence the signal level of the Rayleigh wave through the period range from 40 to 100 sec is not so different, and the waves can be used

for the phase velocity determination up to 100 sec.

The seismograms shown in Fig. 11 were Fourier analyzed and the phase spectra are shown in Fig. 12. The total initial phase of Rayleigh waves, composed of the space phace (6), the rupture propagation phase (13) and the time phase (15), is shown in the figure together with the WWSSN instrumental phase delay calculated through the formula by HAGIWARA (1958). The phase variations of both the total initial phase and the instrument are extremely weak compared with those of the observed waves.

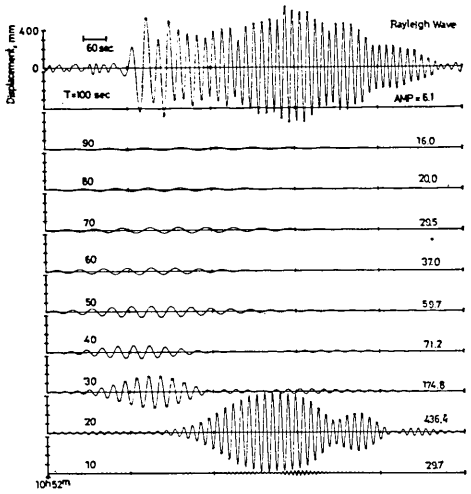

Fig. 11. Rayleigh waves recorded at RAR (uppermost) and the band-pass filtered seismograms for the cente periods (T) from 100 to 10 sec every ten seconds. *AMP* indicated in the right hand side means the maximum half amplitude of the band-pass filtered seismogram.

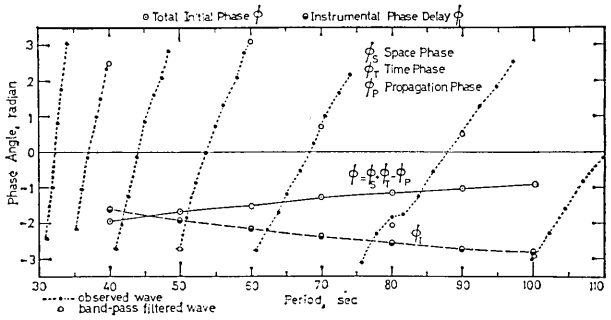

Fig. 12. Phase spectra of Rayleigh waves observed at RAR, total initial phase, and instrumental phase delay.

Phase velocity of Rayleigh waves over the path length of 9018 km in the west Pacific was obtained from the expression

$$c(p)=\frac{pr}{t_0+\{\phi'-(\phi+\phi_I+2n\pi)\}/p} \tag{19}$$

where c: phase velocity,
ϕ: total initial phase,
ϕ_I: instrumental phase delay,
ϕ': observed phase angle indicated by open circles Fig. 12,
r: epicentral distanee,
n: integer number,
t_0: fiducial origin on seismograms.

In Fig. 13 the calculated phase velocity is shown together with the group velocity calculated independently by means of the multiple filtering anal-

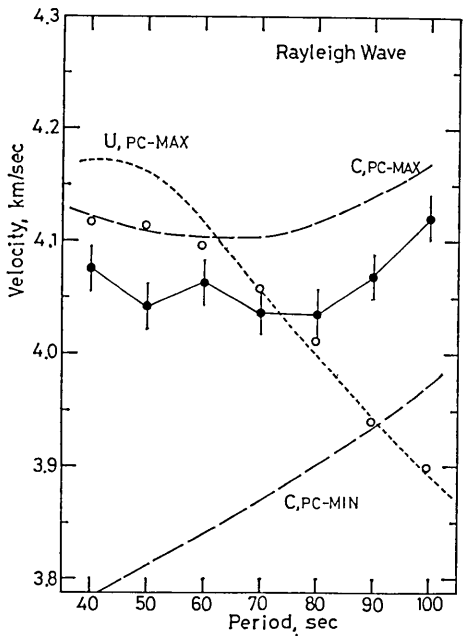

Fig. 13. Calculated phase velocities (solid circles) for the period range from 40 to 100 sec. Group velocities determined independently by means of the multiple filtering analysis are shown by open circles. Theoretical phase and group velocities calculated for the models PC-MAX and PC-MIN are also shown. Vertical bars attached to the solid circles show the phase velocity error for the path-length error of ±0.5% of 9018 km.

ysis, presenting a smooth curve of the phase velocity except a slightly higher value at the period 60 sec. For the determination of velocities the phase and group velocity curves calculated for the models PC-MAX and PC-MIN, which represent the upper and lower limits of velocity in the Pacific, were referred to.

From Fig. 13 we see a feature that the phase velocity is lower than the group velocity in a period range from 40 to 80 sec. This is a typical dispersion characteristic of the fundamental mode Rayleigh waves in the western Pacific, and is never observed in Rayleigh waves travelling the continent or other oceans. The generation of such a distinctive feature seems to be attributed to the underground structure in the western Pacific which is inferred to be composed of the old and thick lithosphere and the well-developed low velocity zone (LVZ).

The wavelength of Rayleigh waves, about 160 and 400 km at 40 and 100 sec respectively, suggests that the wave near 40 sec is mostly controlled by the oceanic old lithosphere and that near 100 sec by the LVZ expanding in the depth of about 100 to 200 km, where mantle materials such as olivine or dunite are partially melted. The upper mantle structure under the western Pacific is principally characterized by the rigidity contrast in the oceanic lithosphere, the LVZ and the layer below the LVZ. In the model PC-MAX the rigidity in the LVZ is about 6.4×10^{11} dyne/cm^2, in the layers shallower and deeper than the LVZ is one order of magnitude higher than the value in the LVZ.

In the present analysis the epicenter location reported by USGS was employed. The formula (19), however shows that the phase velocity is directly affected by the accuracy of the epicentral distance. If we use ISC reports the epicentral distance to RAR is 7 km less (0.08% of 9018 km), which corresponds to the velocity error of approximately 0.003 km/sec for the period range considered here, and is extremely small and negligible. For the determination of surface wave velocity over the Pacific, the epicentral distance usually ranges from 5000 to 10000 km. The probable distance error will be, in the worst case, about 20 km, hence the accuracy of the phase velocity is estimated to be within 0.01 km/sec or so for the Pacific path. The expression (19) indicates that the distance error affects strongly the velocity resolution for the short-path length.

According to USGS and ISC reports (Table 1), the difference in the origin time is 2.7 sec, which corresponds to the phase velocity difference of 0.005 km/sec. When there is an error of 5 sec in the origin time, the phase velocity error approaches up to 0.009 km/sec. This error is not small.

8. Accuracy of the phase velocity of Rayleigh waves

As was examined in the previous sections the space phase error due to the selection of the medium model and source parameter errors is small, if 1) the reasonable model for the location of earthquake is used, 2) the error of the source parameters such as the dip and slip angles is $\pm 3^\circ$ or less, and 3) the station is selected to avoid the minimum amplitude azimuth.

For the period longer than 40 sec, the time phase error is also small even if we assume a step-function as the source time function, insofar as the earthquake of magnitude 6 or less is employed. The disregard of the propagation phase, which is usually done in the single-station method, seems to become a large error factor, particularly when we use the earthquake with magnitude about 6 whose fault length is abnormally longer than expected empirically from the magnitude-fault length relation as expressed in (14).

Instrumental phase delay is accurately calculated if we know the seismograph constants, and the phase spectra of the observed surface waves can be also obtained in high accouracy. So far the phase characteristics needed for the single-station method were examined from various angles. It was found that the errors involved in the calculation of the initial phase are estimated to be within 0.3 radian, even in the worst case 0.6 radian.

Table 2. An example of the phase velocity error for the phase error of 0.3 or 0.6 radian when the single-station method is employed.

Period (sec)	Wave Length (km)	Phase Velocity (km/sec)	Phase Error (radian)	Velocity Error (km/sec)	(%)
40	163	4.075	0.3	0.004	0.098
			0.6	0.007	0.172
50	202	4.041	0.3	0.004	0.099
			0.6	0.009	0.223
60	244	4.064	0.3	0.005	0.123
			0.6	0.011	0.271
70	283	4.037	0.3	0.006	0.149
			0.6	0.013	0.297
80	323	4.034	0.3	0.007	0.174
			0.6	0.014	0.347
90	366	4.069	0.3	0.008	0.197
			0.6	0.016	0.393
100	412	4.121	0.3	0.009	0.218
			0.6	0.018	0.437

In the phase velocity determination in the previous sections, the total initial phase composed of the space phase, time phase and propagation phase was completely calculated on the basis of the dislocation parameters of the earthquake. The phase velocity error due to the initial phase errors was estimated by shifting the initial phase by 0.3 and 0.6 radian in the expression (19) and is shown in Table 2. Phase error of 0.3 radian produces a velocity error of 0.004 km/sec (0.1%) at the period 40 sec and 0.009 km/sec (0.2%) at 100 sec. The velocity error for the phase error of 0.6 radian is nearly twice the value for 0.3 radian.

When we use earthquakes with magnitude less than about 6.0, satisfying an empirical relation of the magnitude-fault length as expressed in (14), the phase velocity of surface waves can be determined precisely by means of the single-station method, even if we disregard the fault length in the initial phase. The phase velocity error of Rayleigh waves for the initial phase error of 0.6 radian, for the path length of about 9000 km, will be less than 0.4% for the period range from 40 to 100 sec.

Acknowledgments

The author wishes to thank Profs. T. Usami, T. Maruyama and Dr. R. Yamaguchi for their valuable discussions and suggestions in the early stage of this work. He is also grateful to Profs. M. Saito, M. Ohnaka and T. Yoshii for their valuable suggestions.

References

AKI, K., 1962, Accuracy of the Rayleigh wave method for studying earthquate mechanism, *Bull. Earthq. Res. Inst.*, 40, 91-105.

AKI, K., 1966, Generation and propagation of *G* waves from the Niigata earthquake of June 16, 1964, *Bull. Earthq. Res. Inst.*, 44, 23-88.

AKI, K., 1967, Scaling law of seismic spectrum, *J. Geophys. Res.*, 72, 1217-1231.

AKI, K., 1968, Seismic displacements near a fault, *J. Geophys. Res.*, 73, 5359-5376.

AKI, K., 1972, Scaling law of earthquake source time-function, *Geophys. J. R. Astr. Soc.*, 31, 3-25.

ARCHAMBEAU, C. B., 1968, General theory of elastodynamic source fields, *Rev. Geophys.*, 6, 241-288.

BEN-MENAHEM, A., 1961, Radiation of seismic surface waves from finite moving sources, *Bull. Seism. Soc. Amer.*, 51, 401-435.

BEN-MENAHEM, A. and M. N. TOKSÖZ, 1963, Source mechanism from spectrums of long-period surface waves, 2. The Kamchatka earthquake of November 4, 1952, *J. Geophys. Res.*, 68, 5207-5222.

BROWN, R. D. and J. G. VEDDER, 1967, Surface tectonic features along the San Andreas Fault, *Geol. Surv. Prof. Paper*, 579, 2-23.

BRUNE, J. N., J. E. NAFE and J. E. OLIVER, 1960, A simplified method for the analysis and synthesis of dispersed wave trains, *J. Geophys. Res.*, 65, 287-304.

BURRIDGE, R., 1969, The numerical soution of certain integral equations with non-integrable kernels arising in the theory of crack propagation and elastic wave diffraction, *Phil. Trans. Roy. Soc. London, Ser. A.*, **265**, 353-381.

DZIEWONSKI, A., S. BLOCH and M. LANDISMAN, 1969, A technique for the analysis of transient seismic signals, *Bull. Seism. Soc. Amer.*, **59**, 427-444.

FILSON, J. and T.V. MCEVILLY, 1967, Love wave spectra and the determination of the 1966 Parkfield sequence, *Bull. Seism. Soc. Amer.*, **57**, 1245-1257.

FORSYTH, D.W., 1975a, A new method for the analysis of multi-mode surface wave dispersion: Application to Love-wave propagation in east Pacific, *Bull. Seism. Soc. Amer.*, **65**, 323-342.

FORSYTH, D.W., 1975b, The early structural evolution and anisotropy of the oceanic upper mantle, *Geophys. J.R. Astr. Soc.*, **43**, 103-162.

HAGIWARA, T., 1958, A note on the theory of the electromagnetic seismograph, *Bull. Earthq. Res. Inst.*, **36**, 139-164.

HANSON, M.E., A.R. SANFORD and R.J. SHAFFER, 1971, A source function for a dynamical bilateral brittle shear fracture, *J. Geophys. Res.*, **76**, 3375-3383.

HARKRIDER, D.G., 1970, Surface waves in a multilayered elastic media. Part II. Higher mode spectra and spectral ratios from point sources in a plane layered earth models, *Bull. Seism. Soc. Amer.*, **60**, 1937-1987.

IDA, Y. and K. AKI, 1972, Seismic source time function of propagating longitudinal-shear cracks, *J. Geaphys. Res.*, **77**, 2034-2044.

IIDA, K., 1959, Earthquake energy and earthquake fault, *J. Earth Sci., Nagaya Univ.*, **7**, 98-107.

IIDA, K., 1965, Earthquake magnitude, earthquake fault, and source dimensions, *J. Earth Sci., Nagoya Univ.*, **13**, 115-132.

KANAMORI, H., 1970a, Synthesis of Long-period surface waves and its application to earthquake source studies-Kurile island earthquake of October 13, 1963, *J. Geophys. Res.*, **75**, 5011-5027.

KANAMORI, H., 1970b, The Alaska earthquake of 1964: Radiation of long-period surface waves and source mechanism, *J. Geophys. Res.*, **75**, 5029-5040.

KAUSEL, E.G., A.R. LEEDS and L. KNOPOFF, 1974, Variations of Rayleigh wave phase velocities across the Pacific Ocean, *Science*, **186**, 139-141.

KAWASAKI, I., 1975, On the dynamical process of the Parkfield earthquake of June 28, 1966, *J. Phys. Earth*, **23**, 127-144.

KNOPOFF, L. and F.A. SCHWAB, 1968, Apparent initial phase of a source of Rayleigh waves, *J. Geophys. Res.*, **73**, 755-760.

KUO, J., J.N. BRUNE and M. MAJOR, 1962, Rayleigh wave dispersion in the Pacific Ocean for the period range 20 to 140 seconds, *Bull. Seism. Soc. Amer.*, **52**, 333-357.

LEEDS, A.R., L. KNOPOFF and E.G. KAUSEL, 1974, Variations of upper mantle structures under the Pacific Ocean, *Science*, **186**, 141-143.

LEEDS, A.R., 1975, Lithospheric thickness in the western Pacific, *Phys. Earth Planet. Inter.*, **11**, 61-64.

MARUYAMA, T., 1963, On force equivalents of dynamic elastic dislocations with reference to the earthquake mechanism, *Bull. Earthq. Res. Inst.*, **41**, 467-486.

ODAKA, T. and T. USAMI, 1970, Theoretical seismograms and earthquake mechanism Part III. Azimuthal variation of the initial phase of surface waves. *Bull. Earthq. Res. Inst.*, 48, 669-689.

OHNAKA, M., 1973, A physical understanding of the earthquake source mechanism, *J. Phys. Earth*, **21**, 39-59.

OTSUKA, M., 1965, Earthquake magnitude and surface fault formations, *J. Seism. Soc. Japan, Ser.* II, **18**, 1-8.

PRESS, F., 1967, Dimensions of source region for small shallow earthquakes, *Proceed-*

ings of the VESIAC conference on the current status and future progress for understanding the source mechanism of shallow seismic events in the 3 to 5 magnitude range.

SAITO, M., 1967, Excitation of free oscillations and surface waves by a point source in a vertically heterogeneous earth, *J. Geophys. Res.*, **72**, 3689-3699.

SATÔ, Y., 1960, Synthesis of dispersed surface waves by means of Fourier transform, *Bull. Seism. Soc. Amer.*, **50**, 417-426.

SCHLUE, J.W. and L. KNOPOFF, 1976, Shear wave anisotropy in the upper mantle of the Pacific basin, *Geophys. Lett.*, **3**, 359-362.

SCHLUE, J.W. and L. KNOPOFF, 1977, Shear-wave polarization anisotropy in the Pacific basin, *Geophys. J.R. Astr. Soc.*, **49**, 145-165.

SHIMAZAKI, K., 1975, Low-stress-drop precursor to the Kurile Islands earthquakes of August 11, 1969, *Trans. Amer. Geophys. Union*, **56**, 1028.

TOCHER, D., 1968, Earthquake energy and ground breakage, *Bull. Seism. Soc. Amer.*, **48**, 147-153.

TSAI, Y.B. and K. AKI, 1970, Precise focal depth determination from amplitude spectra of surface waves, *J. Geophys. Res.*, **75**, 5729-5743.

WU, F.T., 1968, Parkfield earthquake of June 28, 1966: Maginitude and source mechanism, *Bull. Seism. Soc. Amer.*, **58**, 689-709.

WYSS, M. and J.N. BRUNE, 1968, Seismic moment, stress, and source dimensions for earthquakes in the California-Nevada region, *J. Geophys. Res.*, **73**, 4681-4694.

YAMASHITA, T., 1977, Dependence of source time function on tectonic field, *J. Phys. Earth*, **25**, 419-445.

YOSHIDA, M., 1977, Initial phase and phase velocity of surface waves, *Bull. Earthq. Res. Inst.*, **52**, 343-355.

YOSHIDA, M., 1978, Group velocity distributions of Rayleigh waves and two upper mantle models in the Pacific Ocean. *Bull. Earthq. Res. Inst.*, **53**, 319-338.

YOSHIDA, M., 1982, Spectra of the first higher mode of simulated oceanic Rayleigh waves generated by deep earthquakes of the dip-slip type, *Bull. Earthq. Res. Inst.*, **57**, 609-625.

YOSHII, T., 1975, Regionality of group velocities of Rayleigh waves in the Pacific and thickening of the plate, *Earth Planet. Sci. Lett.*, **25**, 305-312.

29. 表面波の初期位相と位相速度の精度
—特に一観測点法に関連して—

地震研究所　吉田　満

震源の深さ，型，方向性，震源時間関数，震源近傍の媒質の属性等，地震の震源パラメータに依存する表面波の初期位相が特に精度に関連して研究されている．地震メカニズム解の小さな誤差や震源近傍の局地的な地下構造の不確定さが表面波の初期位相に及ぼす効果が転位理論に基いて定量的に調べられている．

震源パラメータの誤差を仮定し，異なる媒質モデルを使う事により，初期位相と表面波速度の誤差が計算されている．震源に於ける断層面の傾斜角と滑り角の ±5° の誤差に対して初期位相の空間位相の誤差は，最小振幅方向を除けば，多くの所で無視し得る．震源時間関数の誤差に対しては，0.1 ラジアン前後の位相角誤差が周期40秒で生じ，かつその誤差は周期と共に減少する．もしマグニチュード6の地震を点震源と見做すと，有限な断層の長さによる初期位相の誤差，最大で0.4ラジアンの誤差が破壊伝播方向と丁度反対の方位角度で生じるであろう．震源近傍の媒質の属性の不確定さによる空間位相誤差は，震源域を代表する適当なモデルを使う限りに於て無視し得るといえる．

初期位相の三つの位相因子の中では，破壊伝播位相の誤差が空間位相や時間位相の誤差よりも大であり，初期位相の誤差は周期の増加と共に減少する．マグニチュード6前後の地震が使われ，震源に於ける表面波の振幅ラジエーションパターンが考慮され，かつ観測点が初期位相の安定した所になるような方位であるように注意深く選択されれば，初期位相の総合的な誤差は周期40秒で 0.6 ラジアン，周期100秒で0.3ラジアンを越えないであろうと思われる．

周期40秒と100秒で初期位相の誤差 ±0.6 ラジアンに対して，径路の長さが約 9000 km の場合には，レイリー波の位相速度の誤差はそれぞれ ∓0.007 km/sec (0.17%) と ∓0.018 km/sec (0.44%) に見積られる．